

IN-SITU SATURATION DEVELOPMENT DURING SPONTANEOUS IMBIBITION

B. A. Baldwin and E. A. Spinler
Phillips Petroleum Co., Bartlesville OK, USA

Abstract

The in-situ saturation development for reservoir core plugs has been monitored during spontaneous imbibition using MRI. The images measure both the movement of the front and the saturation change across the front as a function of initial water saturation. At zero initial water saturation the water front exhibited a very steep saturation gradient and after the front passed through a given volume no additional oil was produced from that volume. As initial water saturation was increased the front moved more rapidly, showed less of a saturation gradient and significant oil was produced after the front passed through a given volume. At 33%PV initial water saturation, for a highly-water-wet plug and at 15% PV initial water saturation for a less water-wet plug, no water-front was observed, the oil saturation uniformly decreased everywhere in the core during imbibition. These results suggest two concurrent mechanisms of water influx; one a bulk water displacement of oil and the other a long range process, possibly a thickening of pre-existing water films on the surface. Between the two extremes of initial water saturation the influx of water initially limited the rate of oil production, then when the plug reached a uniform saturation, the transport of the decreasing oil saturation out of the plug became the rate-limiting component.

Introduction

Imbibition has long been considered to be a major contributor for the recovery of hydrocarbons from reservoirs, particularly fractured North Sea Chalk (1-4). Imbibition rate and end point saturation have been found to be a function of rock wettability, the brine's ionic strength, composition and pH and the oil's composition (5-10). From these studies, various mechanisms have been postulated for the transport of water into the pore network during imbibition, however, without information on the in-situ distribution and changes with time it has not been possible to verify these proposals. With the advent of in-situ imaging methods (11-17) it became possible to measure and monitor saturation development with better than 400 micrometer spatial resolution. These techniques provide new information to aid in the evaluation of the proposed imbibition mechanisms.

Experimental

The Magnetic Resonance Imaging, MRI, images were obtained with a Varian 85/310 CSI, which has a 31 cm bore, 2T superconducting magnet and operates at 85.55 Mhz for hydrogen protons. Either a 9 cm or a 12.7 cm I.D. saddle coil was used as the combination transmitter/receiver coil. The coil was matched to sample size. Signals from hydrogen protons were obtained using the Hahn spin-echo sequence. The echo time and recovery time were adjusted to maximize signal intensity; typically echo times were 3 ms and recovery times ranged from 4 to 0.5 sec. The field of view was adjusted to fit the sample but typically was 8 by 9 cm, giving a pixel resolution of 300 to 350 micrometers. The images consisted of 255 levels of gray in a 256 x 256 display. The intensity and contrast of the individual pictures were adjusted to produce a presentable visual display; however, for quantitative determinations absolute intensities were used. Image intensities were transferred to a spreadsheet, where quantitative saturation values were calculated. MRI images reveal the distribution of porosity from the intensity distribution in a fully saturated rock and changes in saturation, as reduced intensity, when the imaged fluid is displaced. In these experiments decane was the imaged fluid. For these clean, chalk plugs the decane's image intensity is proportional to its saturation. Water saturation was determined by subtracting the decane saturation from unity. For chalk, the MRI derived saturation is typically less than +/- 2%PV of the gravimetrically derived saturation. Images were collected as a function of time and animated to enhance visualization of the flow patterns.

The samples consisted of one-inch diameter plugs drilled horizontally from reservoir core. The plugs were cleaned by alternately cycling toluene and methanol in a soxhlet extractor. For varying initial water saturation one plug was used, to minimize the effect of plug to plug variation. Initial water saturation was achieved by placing the cleaned and dried plug in a vacuum chamber and pumping out the air. When the core reached a reasonable vacuum, degassed water was transferred into the chamber and the pressure returned to atmospheric. This procedure was necessary to saturate the small pore spaces with fluids. Subsequent changes in fluid saturation were produced either by centrifuging or pumping a second fluid into the core.

The fluids consisted of deuterium oxide, D₂O (heavy water), which was not imaged with the current parameter set and decane as the hydrocarbon phase, which was imaged. Wettability of the plugs was determined by the Amott method (18).

Results and Discussion

Figure 1 shows water imbibition, at six representative time steps, into 100% decane saturated plug A, $S_{wi}=0\%PV$. The water phase was not imaged and appears black. The plug was supported at four contact points, thus it was completely surrounded by water, making all surfaces available for imbibition. The bright oblong shapes, primarily at the top and bottom of the plug, are expelled decane, which clung to the outside of the plug until the drop become large enough to break away. The decane then floated to the top of the water and produced a bright line across the top of the image that increased in volume with imbibition. Imbibition of 100% decane saturated plugs, for all seven 100% decane saturated experiments, always began at the bottom of the plug. These imbibition experiments included vertical and horizontal configurations and different plugs. This suggested that gravitational forces, although quite small (ca. 0.04 psi for horizontal and 0.06 psi for vertical), are sufficient to initiate imbibition at the bottom of the plug as opposed to any other location. Once imbibition began, water did not enter any other face for more than an hour, even though all faces of this highly water-wet rock were submerged in heavy water. After about 1.5 hours imbibition was observed at several other faces of the plug, Fig. 1D. Although, in the experiment shown, water never entered from the left vertical face. Imbibition for the 100% decane saturated plug proceeded with a strong saturation gradient, as shown in Fig. 4 for the vertically oriented water saturation profiles, across the site of the initial imbibition, as a function of time. By convention these profiles are plotted as water saturation, thus they are the inverse of the images which show decane saturation.

Fig. 2 shows imbibition into plug B with an initial water saturation of 15% PV. Fig. 2A shows the plug before imbibition and Fig. 2B is after approximately 5 minutes of imbibition. The major difference between this experiment and the preceding one, plug A at $S_{wi}=0\%PV$, is that at $S_{wi}=15\%$ imbibition occurred simultaneously at all faces. The reduced rate of imbibition in the plug's upper right corner, most notable by exhibiting a higher decane saturation in Fig. 2C and a slightly brighter area in Fig. 2D, is probably an area of slightly lower permeability. This feature is also visible in the intermediate images, which are not included in Fig. 2. The actual volume of the remaining decane in Figs. 2B and 2C is a cylinder since water entered from all faces. The images in Fig. 2 are 4mm thick, vertical slices through the center of the plug and represent only the decane saturation in this one slice. Horizontal profiles of water saturation through the center of the images, Fig. 5, show the presence of a front that is not quite a steep as those in the $S_{wi}=0\%PV$ imbibition test, Fig. 4 and Table 1. Horizontal profiles were used for this and the higher S_{wi} 's because they had less interference with imbibition from the cylindrical sides of the plug. In addition, after the fronts passed, Fig. 2D and 0.72 hr profile in Fig. 5, imbibition continued without a discernable front. The profiles in Fig. 5 show that until 0.87 hr, the saturation in advance of the front, was unchanged from the initial water saturation, i.e. no decane was displaced from the center of the plug. After 0.87 hr, Fig. 5, decane was displaced through out the plug and water saturation increased accordingly.

Fig. 3 shows decane distribution images with the same plug as above, plug B, at a much higher initial water saturation, $S_{wi}=33\%PV$. The corresponding horizontal profiles are shown in Fig. 7. The general appearance of the images shows virtually no frontal advance. The profiles show a weak saturation gradient near the face and increased water saturation throughout the plug in the first image, ca. 5 minutes. This indicated that water reached the center of the plug while the first image was being produced. These profiles, at high initial water saturation, contrast sharply to the profiles at low initial saturation where the center of the plug was not contacted by water for up to an hour after imbibition began.

Fig. 6 shows the horizontal profiles for plug B at $S_{wi}=22\%PV$. The images, not shown, and these profiles show less of a frontal component and more uniform change in saturation throughout the plug compared to the same plug at lower S_{wi} . However, water did not penetrate to the center of the plug until the third or fourth images, 0.52 hr. Relevant saturation gradients are given in Table 1.

Fig. 8 shows the water saturation profiles during imbibition for a less water-wet, chalk plug C, at $S_{wi}=15\%PV$. Images were not collected for this particular plug. Plug C was cylindrically sealed in epoxy so imbibition occurred only at the two ends, a 2-D imbibition. For this experiment, because it was also used for other testing, the plug was submerged in heavy water for a prescribed time then removed for MRI and other tests. These horizontal saturation profiles, as a function of time, resemble those in the highly-water-wet plug at high initial water saturation, i.e. the water reached the center of this plug and forced out decane within the time needed to generate the first image, if not immediately after submerging the plug. The saturation gradient near the ends of this plug may represent the loss of decane by evaporation while handling the plug between imbibition and imaging.

Fig. 9 shows the average water saturation as a function of time during the imbibition process. The average saturation was obtained from the image by averaging the local saturation values over the entire plug. The shape of these curves is very similar to standard imbibition tests, where the average saturation is determined by the cumulative volume of effluent. The final water saturation was independent of initial saturation, within experimental error. These results suggest that these tests are comparable to previously run imbibitions.

The results in Table 1 compare the rate of frontal movement, saturation gradient and time for the water to reach the center of the plug for the different initial water saturation tests. As the initial water saturation was increased the saturation gradient of the front decreased sharply. At zero initial water the gradient was constant, suggesting a single mechanism of water imbibition. As the initial water saturation increased, the frontal gradient and time for water to reach the middle of the plug both decreased. At high initial water saturation for the highly-water-wet plug and at moderate initial water saturation for the less water-wet plug there was no significant frontal saturation gradient. The almost immediate transport of water to the center of the plug for highly-water-wet plug at $S_{wi}=33\%$ and less water-wet plug at 15% suggests a second mechanism of water transport into the plug. One possible mechanism would be the thickening of existing water films. As initial water saturation increases the films on water wet surfaces increase in thickness. As the films become thicker they also become better connected and are expected to provide decreased resistance to water movement.

These MRI images were used to spatially determine decane saturation development during spontaneous water imbibition and calculate the corresponding water saturation. At 100% decane the existence of water fronts, or banks, show that the rate of transporting water into the core is the limiting step. After the front passed through a specific part of the plug no further change in decane saturation was observed, within our experimental uncertainty, for the plugs at $S_{wi}=0\%$. This suggests that at zero initial water saturation, imbibition is governed by a single mechanism, probably determined by local capillary forces. At $S_{wi}=15\%$ water fronts formed from imbibition at all exposed faces and moved generally toward the center of the plug. The fact that a water front was still observed implies that oil was expelled faster than water could imbibe into the plug through the pore network. However, unlike the zero initial water saturation case, after the fronts passed a specific location the decane saturation continued to decrease, but at a more uniform saturation distribution. This implies that behind the front, the water had a higher rate of transport than the oil. At $S_{wi}=33\%$ no measurable fronts were observed, the decane saturation decreased uniformly over the whole plug. This indicates that at 33% initial water the rate of water transport was greater than the rate oil transport at an oil saturation of 66%. The lack of a water front indicates a mechanism that is different than in the lower initial water saturation cases. One suggestion that is consistent with the uniform change in saturation throughout the plug is a thickening of pre-existing water films. The reduced wettability in the less water-wet plug apparently shifted the saturation at which the water's transport rate was greater than the oil's, to lower water saturation. This is based on the lack of a water front during imbibition at $S_{wi}=15\%$ in the less water wet plug. The decrease in the rate of oil production with increasing water saturation, Fig. 9, after the front passed, reflects the continued decrease in the oil's transport rate with decreasing oil saturation.

Conclusions

Spontaneous imbibition is an important mechanism for recovery of hydrocarbons, particularly in low permeability fractured chalk

At low initial water saturation the presence of significant water fronts during spontaneous water imbibition indicates that the rate of water transport is less than oil

At high initial water saturation the more uniform saturation change during spontaneous water imbibition indicates that the rate of water transport is greater than oil

The pattern of spontaneous imbibition is dependent on sample wettability, with less effect from frontal movement in less water-wet samples

These experimental models can be used to verify mathematical models of imbibition

Acknowledgment

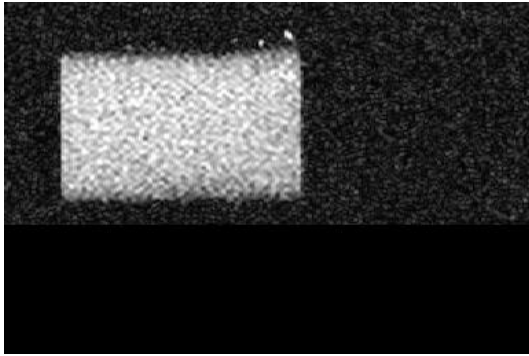
The authors acknowledge permission from Phillips Petroleum to publish this paper. We also thank R.L. King and J.C. Stevens for help with collecting and analyzing the MRI data.

References

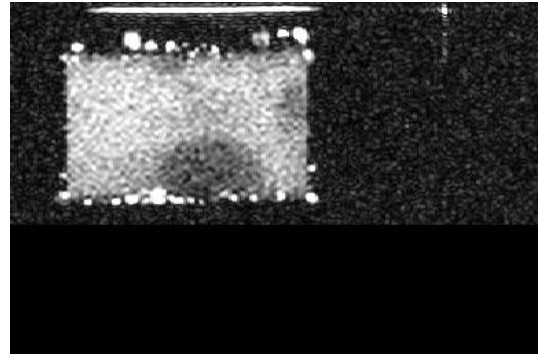
1. Torsaeter, O., "An Experimental Study of Water Imbibition in Chalk from the Ekofisk Field", SPE preprint 12688 presented at the SPE/DOE Fourth Symposium on EOR, Tulsa, OK (April 1984).
2. Weseloh, C.J., "Brine Imbibition and Wettability Behavior of the Ekofisk Field", North Sea Chalk Research Symposium, Stavanger, Norway, (1985) **1**, Paper # 8.
3. B. A. Baldwin, "Water Imbibition and the Characterization of North Sea Chalk Reservoir Surfaces", SPE Formation Evaluation. (1988) **3** 125-30.
4. Torsaeter, O., "An Experimental Study of Water Imbibition in Chalk from the Ekofisk Field", SPE preprint 12688 presented at the SPE/DOE Fourth Symposium on EOR, Tulsa, OK (April 1984).
5. Gunlikson, R.D. and Wier, D.R., "Laboratory Studies on Water Imbibition in Ekofisk" North Sea Chalk Research Symposium, Stavanger, Norway, (1985) **3**, Paper # 5.
6. Graue, A., Viksund, B.G. and Baldwin, B., "Oil Recovery as a Function of Wettability in Low-Permeable Outcrop Chalk", SPE preprint 38896 presented at the 1997 SPE Annual Technical Conference and Exhibition, San Antonio, Tx, Oct. 5-8 (1997); to be published SPEJ (March 1999).
7. Viksund, B.G., Graue, A., Baldwin, B. and Spinler, E., "2-D Imaging of Waterflooding a Fractured Block of Outcrop Chalk", Proc.: 5th Chalk Research Symposium, Reims, France. (7-9 Oct 1996).
8. Ma, S., Morrow, N.R. and Zhang, X., "Generalized Scaling of Spontaneous Imbibition Data for Strongly Water-Wet Systems", J. Petr. Sci. and Eng. (1997) **18**, 165-78.
9. Tang, G.Q. and Morrow, N.R., "Salinity, Temperature, Oil Composition and Oil Recovery by Waterflooding", SPE Res. Engr. (1997) 269-276.
10. Viksund, B.G., Morrow, N.R., Ma, S., Wang, W., and Graue, A., "Initial Water Saturation and Oil Recovery from Chalk and Sandstone by Spontaneous Imbibition" paper SCA-9851, presented at the 1998 SCA International Symposium, The Hague, Sept. 14-16.
11. Lauterbur, P.C. "Image Formation by Induced Local Interactions: Examples Employing Nuclear Magnetic Resonance", Nature (1973) **242**, 190-91.
12. Mansfield, P. and Morris, P.G. "NMR Imaging in Biomedicine" (Academic Press, NY, 1982).
13. Rothwell, W.P. and Vinegar, H.J. "Petrophysical Applications of NMR Imaging", Applied Optics (1985) **24**, 3969-72.
14. Baldwin, B.A. & Yamanashi, W.S. "Detecting Fluid Movement and Isolation

Table 1**Plug results and profile evaluation**

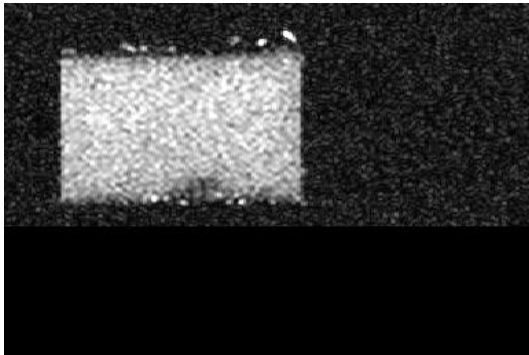
Plug #	Por. (%)	Perm. (md)	Amott Index	Swi (%PV)	Swf (%PV)	Sat. Grad. (fractional sat./cm)	Time for water to reach center
A	29	0.15	1.0	0	60	2.2 All images	1.25 hr
B	24	0.28	1.0	15	67	1.5 Image 1 to 5 0.6 10th image	0.76 hr
B	24	0.28	1.0	22	62	1.0 1st image 0.5 3rd image	0.52 hr
B	24	0.28	1.0	33	69	0.1-0.7 1st image	<0.07 hr
C	33	2.4	0.5	15	49	none	<0.07 hr



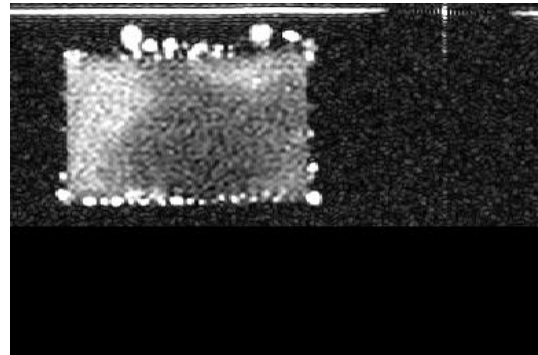
A



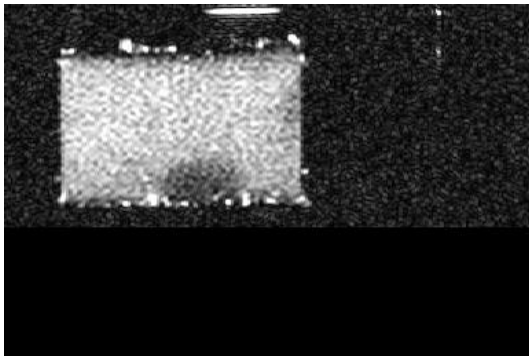
D



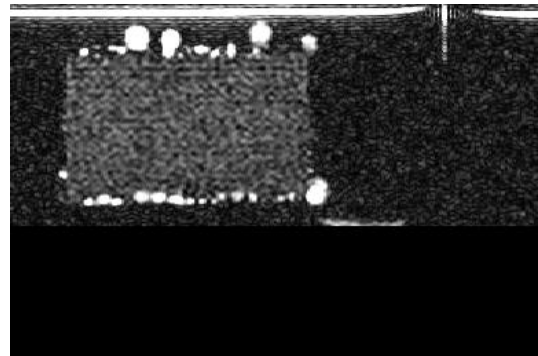
B



E

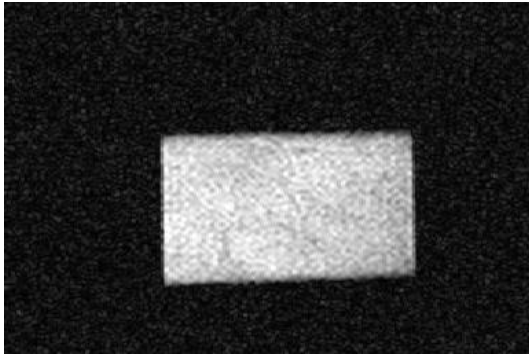


C

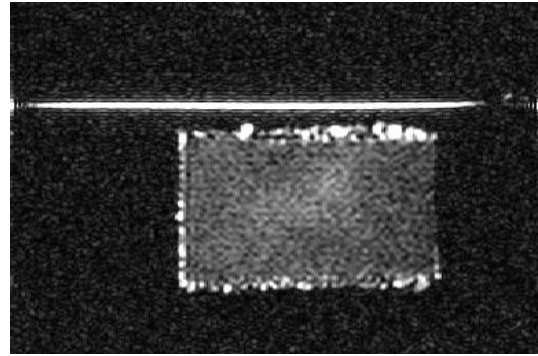


F

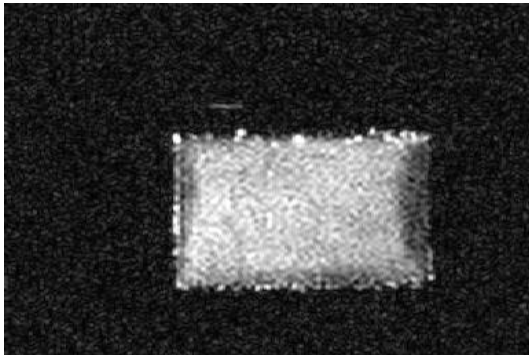
Fig. 1 Spontaneous Imbibition of water into a 100% hydrocarbon/ 0% water saturated chalk plug. Imbibition time increases from A to F.



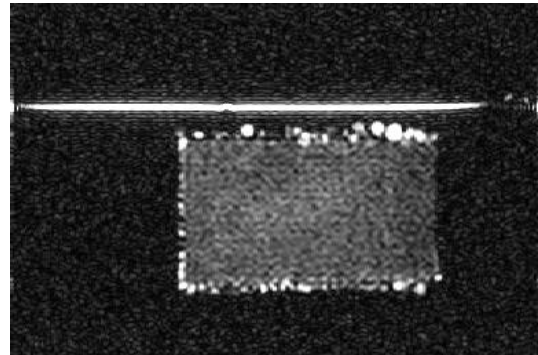
A



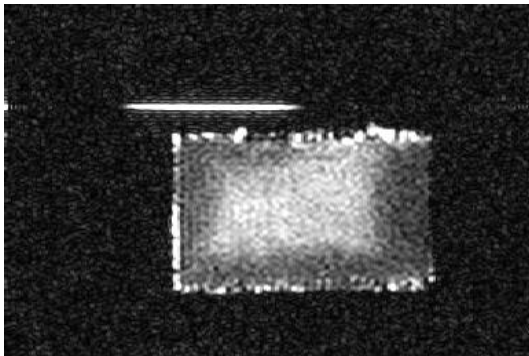
D



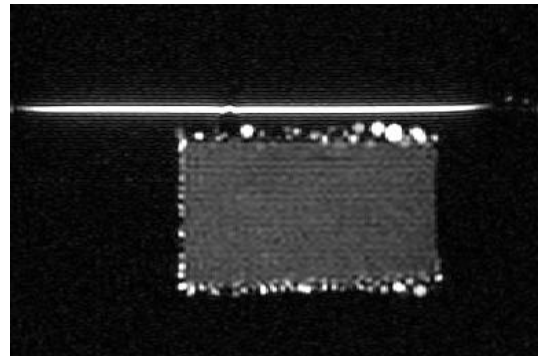
B



E

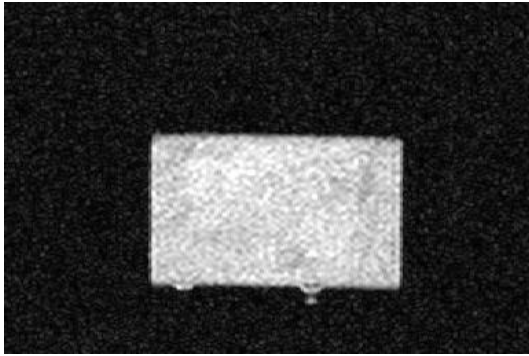


C

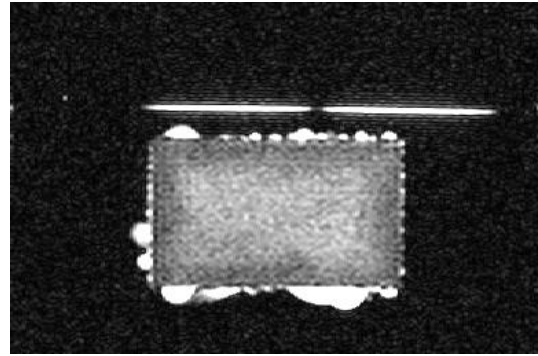


F

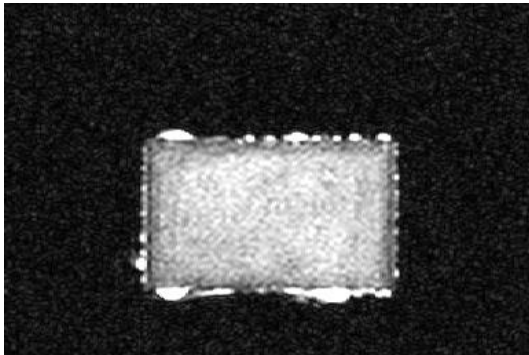
Fig. 2 Spontaneous Imbibition of water into an 85% hydrocarbon/ 15% water saturated chalk plug. Imbibition time increases from A to F



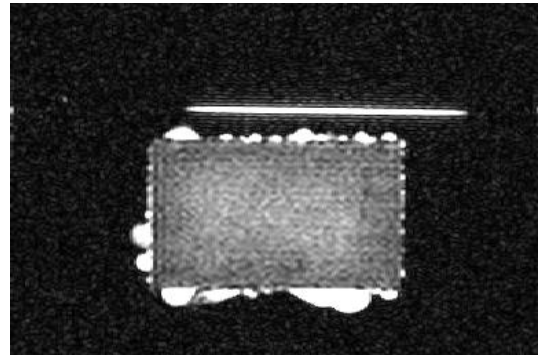
A



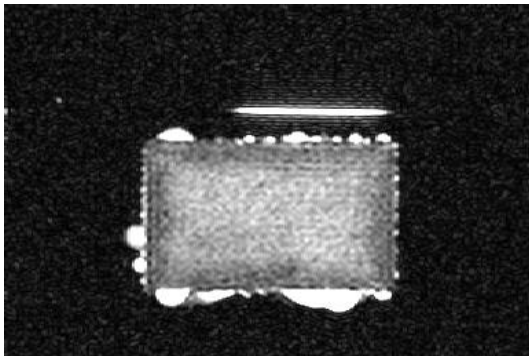
D



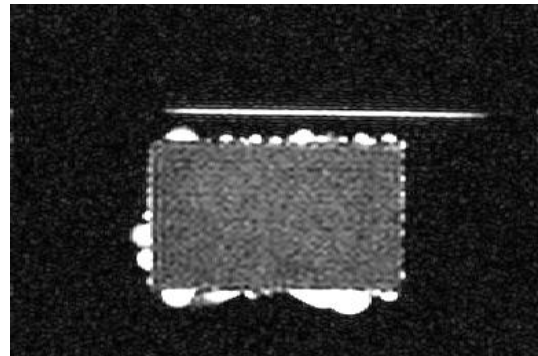
B



E



C



F

Fig. 3 Spontaneous Imbibition of water into a 67% hydrocarbon/ 33% water saturated chalk plug. Imbibition time increases from A to F.

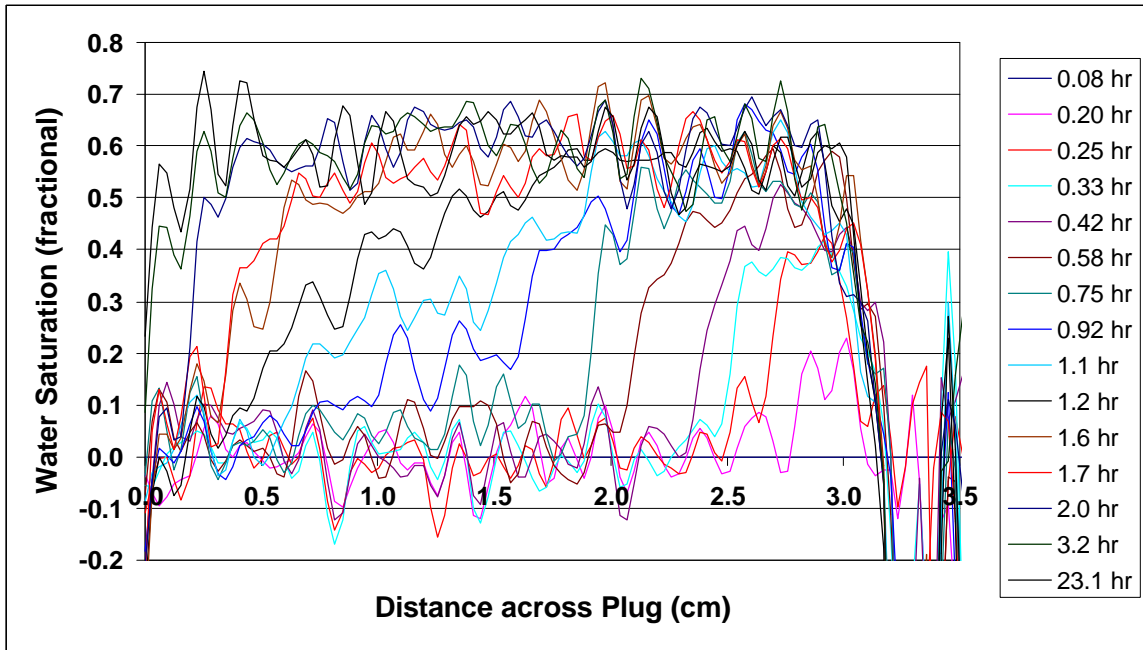


Fig. 4 Vertical profiles during imbibition in plug A at Swi=0%

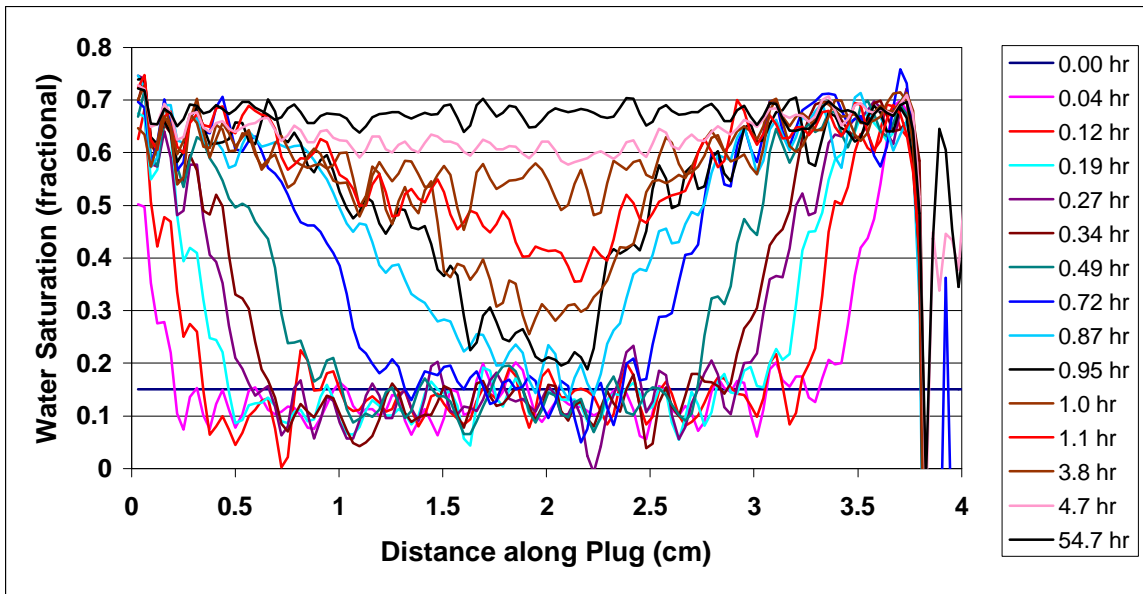


Fig. 5 Horizontal profiles during imbibition in plug B at Swi=15%

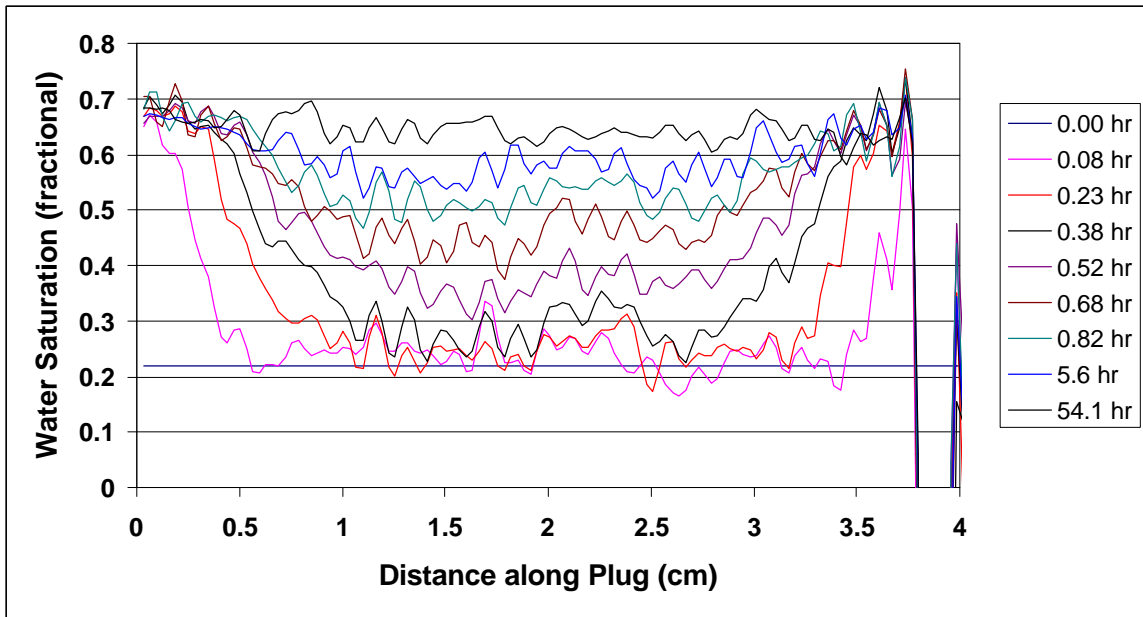


Fig. 6 Horizontal profiles during imbibition in plug B at $S_{wi}=22\%$

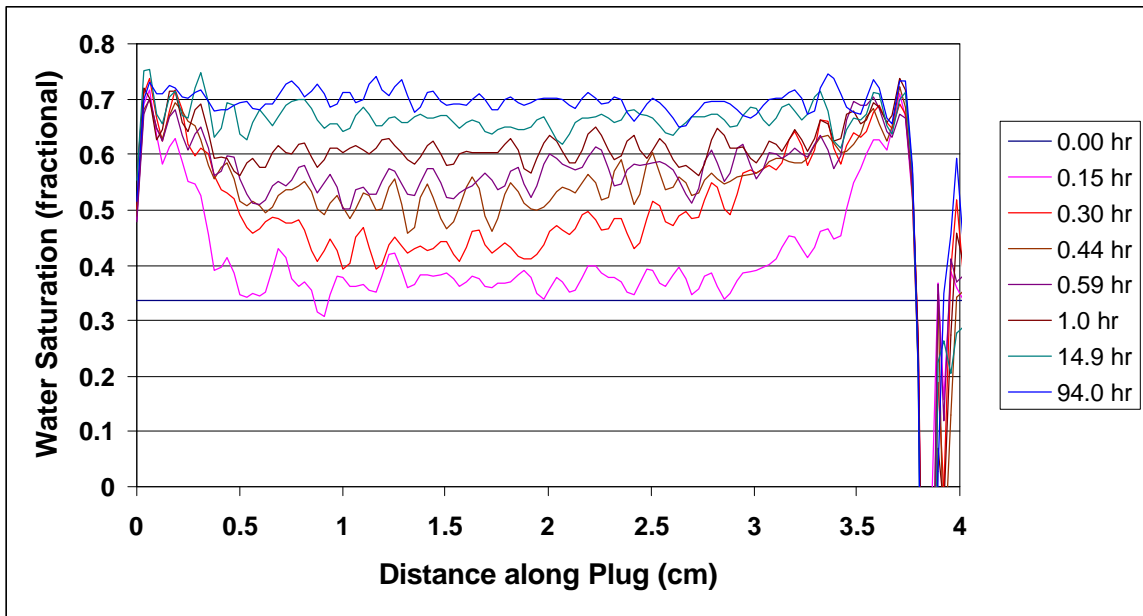


Fig 7. Horizontal profiles during imbibition in plug B at $S_{wi}=33$

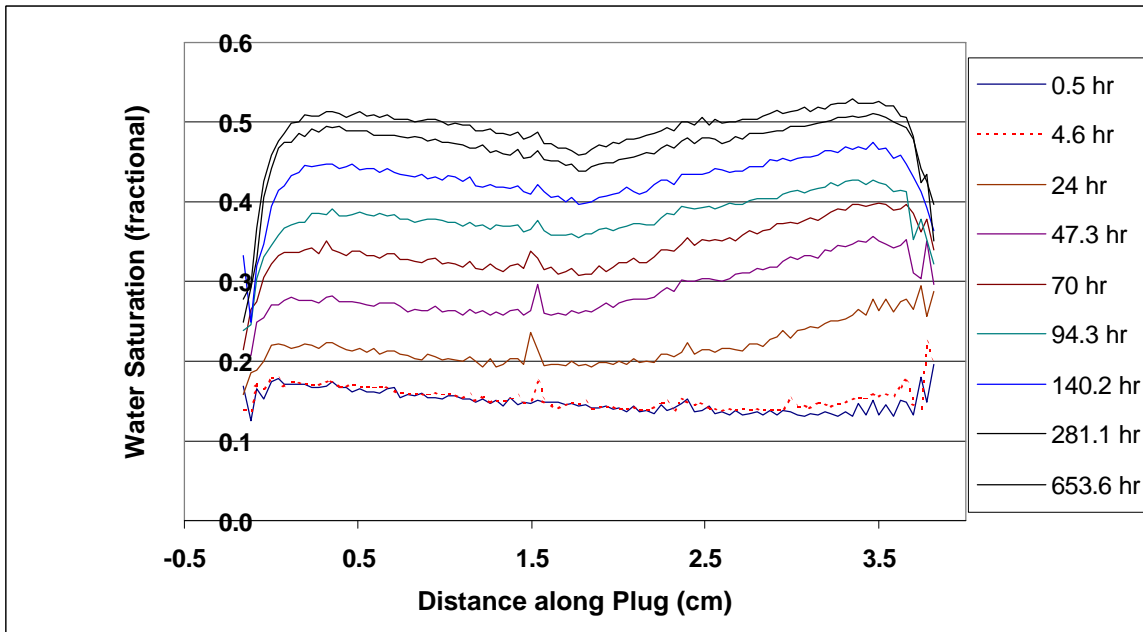


Fig. 8 Horizontal profiles during imbibition for less water-wet plug C at $S_{wi}=15\%$

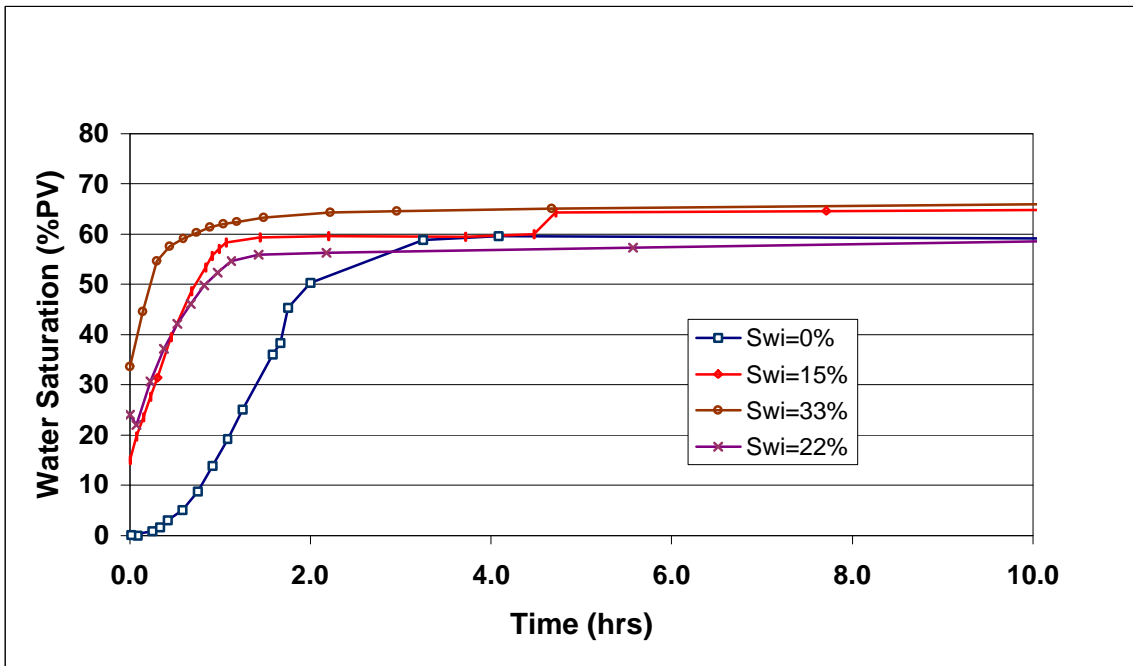


Fig. 9 Cumulative imbibition for several initial water saturations